Emergent Conformational Preferences of a Self-Assembling Small Molecule: Structure and Dynamics in a Tetrameric Capsule

Fraser Hof, Colin Nuckolls, Stephen L. Craig, Tomás Martín, and Julius Rebek, Jr.*

Contribution from the The Skaggs Institute for Chemical Biology and Department of Chemistry, The Scripps Research Institute, 10550 North Torrey Pines Road, La Jolla, California 92037

Received June 28, 2000

Abstract: Herein we report the synthesis of a molecule that self-organizes through hydrogen bonds into discrete tetrameric capsular species, encapsulating large polycyclic guest molecules. The unique folded structure of the assembled state is determined by correlation spectroscopy in conjunction with molecular modeling. Pendant methoxyl groups are essential for the assembly process and convey their influence through both electronic pathways and surface interactions. Spin polarization transfer experiments show that the capsule undergoes rapid guest-exchange processes while being itself kinetically stable at elevated temperatures.

Introduction

Reversible assembly of self-complementary molecules is the method by which Nature constructs its most spectacular structures: allosteric enzymes, membranes and their channels, and viral capsids. These structures inspire the synthesis of smaller molecules which, when several copies interact, show an emergent function−often planned, sometimes unpredicted, but always welcomed. Synthetic assemblies are not so much models of biological structures as they are tests of the architect's intuition, synthetic abilities, and interpretive skills. A passing grade results in progress for the understanding of molecular recognition.

The goal of the research described here is to assemble from self-complementary units capacious host structures that completely surround smaller guest molecules. The formula for assembly is written in hydrogen-bonding preferences, molecular curvature, and the filling of space. The first level of instruction is the molecular recognition via hydrogen bonds of lactam and sulfonamide functionalities. Both units are self-complementary and can form homodimers, but their prejudice is to pair as heterodimers (Figure 1A).[1] The complementarity becomes self-complementarity when a covalent bond links the sulfonamide and lactam recognition units. While a linear linker gives rise to polymeric systems, a higher level of instruction−curvature determines if and where the ends meet. The curvature must be expressed in three dimensions if a closed-shell surface is to be assembled. One of the simplest ways to do so involves doubling the recognition elements at both ends of the linker: sulfamide and glycoluril functionalities are the result (Figure 1B−D).

The combination of these features about a central benzene spacer results in molecules that self-assemble into tetrameric capsules whose cavities (∼160 Å^3) are suited for encapsulation of small cyclic guest molecules (Figure 2A).[1b] Derivatives of these molecules are able to discriminate between enantiomeric guests in solution and are also effective in the construction of dynamic combinatorial libraries.[2]

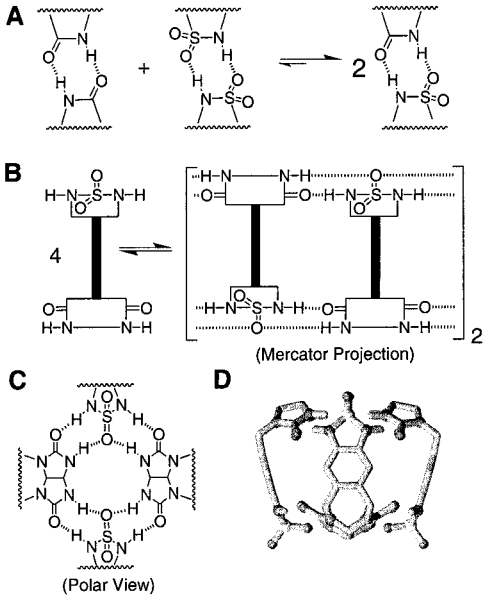

Figure 1. (A) Hydrogen bonding preferences of amide and sulfamide functionalities expressed as an equilibrium. (B,C) Complementary ditopic amide and sulfamide functionalities are connected by a linker that establishes appropriate curvature. The result is a closed-sphere assembly, here viewed as a Mercator projection and along the polar symmetry axis. (D) Molecular model of the spherical assembly that forms when the linker is benzene.[1b] Some hydrogen atoms and substituents have been omitted for clarity.

To expand the dimensions (and the utility) of these capsules a more extended aromatic skeleton is required. We report now the synthesis and characterization of a molecule with a naphthalene spacer with peripheral methoxyl substituents **(1)** and without **(2)** (Figure 2B). The influence of this seemingly subtle structural difference far exceeded our "architect's intuition". The former spontaneously assembles to form tetrameric capsules capable of encapsulation of large polycyclic molecules, while the latter does not form discrete assemblies at all. The

(1) (a) Castellano, R. K.; Kim, B. H.; Rebek, J., Jr. *J. Am. Chem. Soc.* **1997**, *119*, 12671−12672. (b) Martín, T.; Obst, U.; Rebek, J., Jr. *Science* **1998**, *281*, 1842−1845.

(2) (a) Nuckolls, C.; Hof, F.; Martín, T.; Rebek, J., Jr. *J. Am. Chem. Soc.* **1999**, *121*, 10281−10285. (b) Hof, F.; Nuckolls, C.; Rebek, J., Jr. *J. Am. Chem. Soc.* **2000**, *122*, 4251−4252.

10.1021/ja002340q CCC: $19.00
Published on Web 10/21/2000

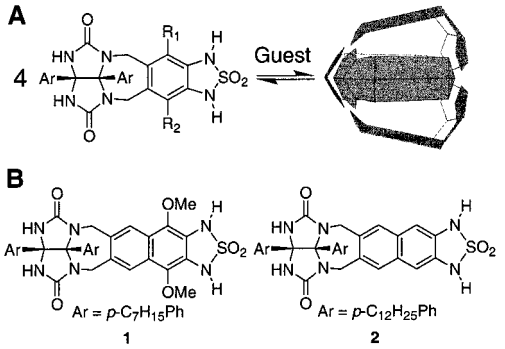

Figure 2. (A) Self-assembly of compounds bearing a benzene spacer between sulfamide and glycoluril gives rise to tetrameric capsules that encapsulate small cyclic molecules. (B) Compounds bearing sulfamide and glycoluril separated by a naphthalene spacer.

self-assembly of **1** is accompanied by a folding process that alters the conformational preferences of the monomer and reduces symmetry in the assembled state. The unique pinwheel-like structure of these tetramers emerges from NOE experiments. The dynamics of self-assembly and guest-exchange processes are characterized through spin polarization transfer (EXSY) experiments.

Synthesis

The key transformation in the synthesis of **1** (Scheme 1) is homologation of the aromatic skeleton. Conversion of known dibromide **3**[2b] to the cyclic sulfinate **4** allowed for mild generation of the *o*-quinodimethane **5**.[3] In situ Diels−Alder reaction followed by oxidation gives the homologated aromatic compound **6**. Reduction gives diol **7**, and bromination gives dibromide **8**. Alkylation of glycoluril **9**[4] with the dibromide **8** followed by deprotection gives the final compound **1**. Compound **2** was prepared by an analogous route from known dibromide **11**.[1b]

Results and Discussion

Compound **1** is monomeric in solvents such as THF, DMF, and DMSO that are effective in competing for hydrogen bond donors. For assembly into discrete tetrameric capsules a noncompetitive solvent and a suitable guest are required. When the capsule forms, the chemical shifts of hydrogen-bonded sulfamide N−H signals are located downfield in the NMR spectra relative to those of the unassembled monomer, and all signals are concentration-independent. Resonances for encapsulated guest are observed upfield of the free guest by ∼1−2 ppm, indicating shielding by the aromatic walls of the host. The exchange of free and encapsulated guest is slow on the NMR time scale at 600 MHz. Integration of signals for encapsulated guest and capsule show the 4:1 stoichiometry expected of the proposed tetrameric assembly surrounding a single guest molecule.

A number of large polycyclic molecules were found to act as guests for the host assembly $\mathbf{1}_4$. Shown in Figure 3 are the NMR spectra that result from encapsulation of 1,3,5,7-tetramethyladamantane [C_{14}] **(12)**, congressane [C_{14}] **(13)**, and (+)-longifolene [C_{15}] **(14)**. Calculations predict the volume[5] of the capsule to be approximately 270 Å^3, as compared to ∼160 Å^3 for other members of the tetramer family. Guests fill 65−80% of the total volume.[6] The binding constants (K_{app}) of some guests (relative to CD_2Cl_2) are reported in Table 1.[7]

The protons of **1** display an unexpected doubling of signals in the assembled state, indicating that the formation of the capsule $\mathbf{1}_4$ results in a loss of symmetry with respect to the unassembled monomer (Figure 3). Molecular models indicate that the methoxyls that fret the cavity are too sterically crowded to rest in the plane of the aromatic spacer. They can be directed either into the cavity or outward to the solvent.[5] 2D-ROESY experiments show through-space NOE contacts between the

Scheme 1: Synthesis of **1** and **2**[a]

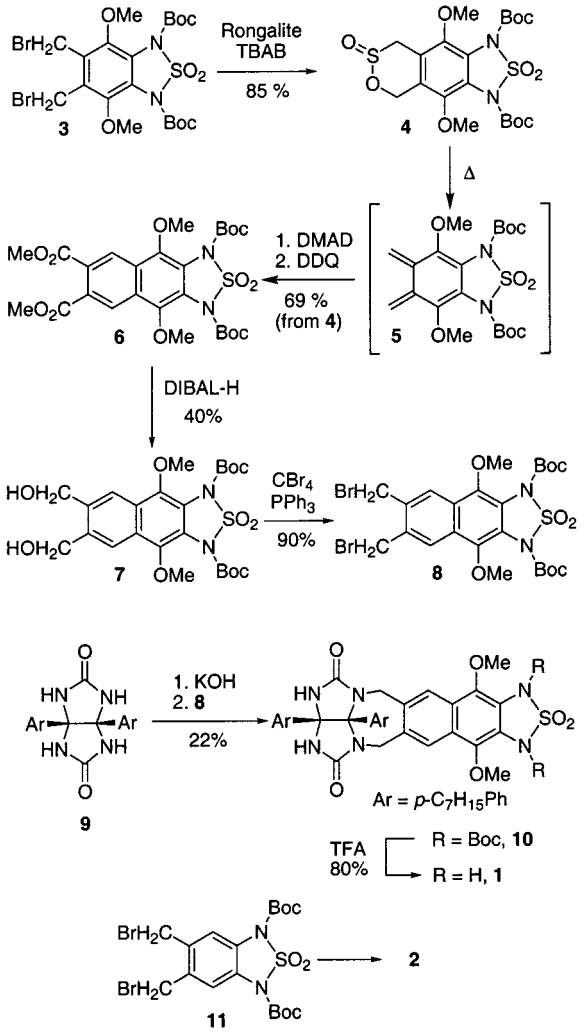

[a] Rongalite = sodium formaldehydesulfoxylate dihydrate, TBAB = tetrabutylammonium bromide, DMAD = dimethylacetylenedicarboxylate, DDQ = 2,3-dichloro-5,6-dicyano-1,4-benzoquinone.

(3) Zhu, Z.; Drach, J. C. Townsend, L. B. *J. Org. Chem.* **1998**, *63*, 977−983.

(4) Kang, J.; Hilmersson, G.; Santamaria, J.; Rebek, J., Jr. *J. Am. Chem. Soc.* **1998**, *120*, 3650−3656.

(5) Molecular modeling of assemblies was carried out using MacroModel 6.5 and the Amber* force field: Mohamadi, F.; Richards, N. G. J.; Guide, W. C.; Liskamp, R.; Lipton, M.; Caufield, C.; Chang, G.; Hendrickson, T.; Still, W. C. *J. Comput. Chem.* **1990**, *11*, 440−467. Cavity volumes of minimized structures were calculated with the GRASP program: Nicholls, A.; Sharp, K. A.; Honig, B. *Proteins* **1991**, *11*, 281−296.

(6) The upper value (80%) is greater than the occupancy factor of closely packed spheres (74%). It is likely that the flexibility and breathing of the assembly are not well represented by the models that lead to this figure. Mecozzi, S.; Rebek, J., Jr. *Chem. Eur. J.* **1998**, *4*, 1016−1022.

(7) K_a(app) is defined from the equilibrium:

$$H_{aggregate} + G \overset{K_a(app)}{\rightleftharpoons} H_4{\cdot}G$$

where H = the host molecule and G = the guest molecule. A detailed description of the method used to calculate K_a(app) from direct integration and from competition experiments is given in ref 1b.

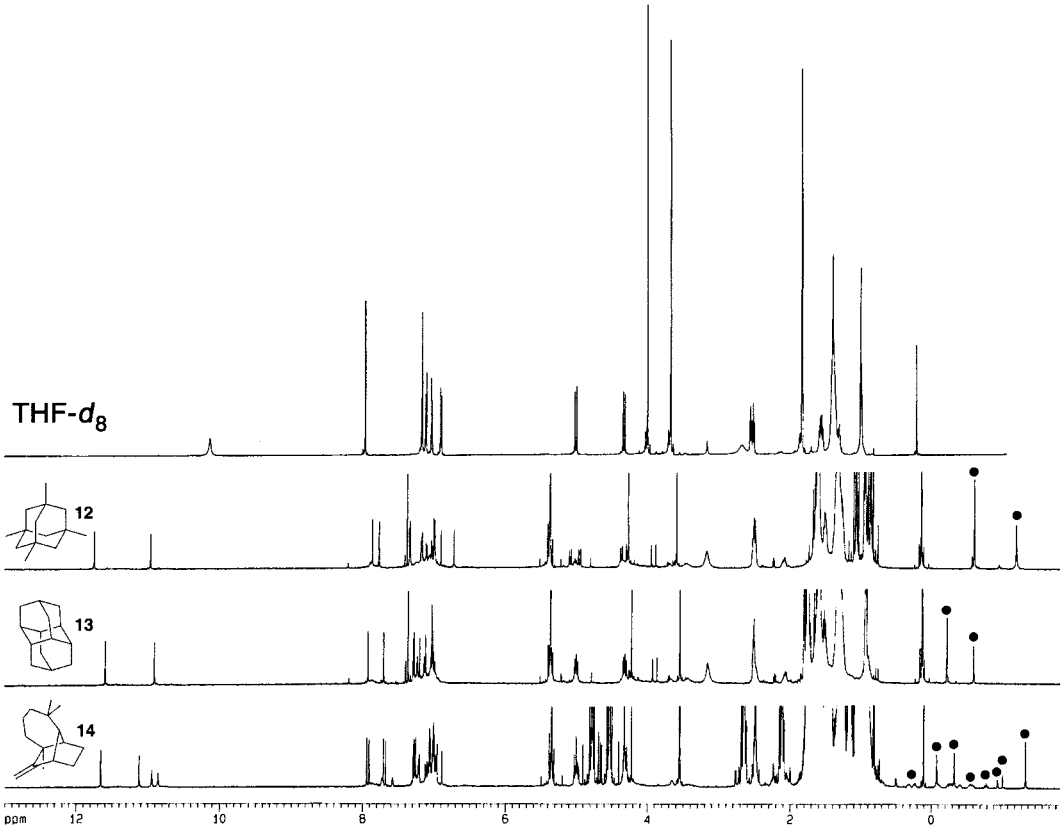

Figure 3. (A) ^{1}H NMR spectra of compound **1**, monomeric in THF-d_8. ^{1}H NMR spectra of assemblies formed by **1** in the presence of a suitable guest in CD_2Cl_2. (B) 15 equiv (with respect to tetramer) of **12**. (C) 15 equiv of **13**. (D) 130 equiv of **14**. The chiral guest results in the expected doubling of signals relative to complexes formed by achiral guests. Signals for encapsulated guests visible in the upfield region are marked with a (●). In all cases, integration of signals for encapsulated guest and capsule give the 4:1 ratio expected of the tetrameric structure encapsulating a single guest.

Table 1: Binding Constants for Complexes of Polycyclic Molecules with **1** and Calculated Volumes of Guest Molecules[a]

guest	K_a(app) (M^{-1})	volume (Å^3)[b]
congressane **(13)**	99[c]	187
1,3,5,7-tetramethyladamantane **(12)**	42[d]	213
(+)-longifolene **(14)**	4.2[c]	222
(1*R*)-(+)-camphor **(15)**	1.4[c]	140

[a] The calculated volume of the cavity of $\mathbf{1_4}$ is 270 ± 10 Å^3. Optimum binding within this series occurs at an occupancy factor of ~70%. Molecules with a volume <140 Å^3 did not exhibit binding. [b] Volumes calculated using GRASP.[5] [c] Apparent binding constants measured by competition experiment.[7] Estimated error is ± 10%. [d] Apparent binding constant measured by direct integration of free and bound guest species.[7] Estimated error is ±10%.

encapsulated guest and only one of the two chemically inequivalent methoxyl groups, indicating that one methoxyl in the assembly is much closer to the encapsulated guest than the other (Figure 4).

Two structures that satisfy the requirements of both molecular modeling and the observed ^{1}H NMR spectra are shown in Figure 5. Structure A is of S_4 (C_{4h}) symmetry, while structure B is a member of the C_{2v} symmetry group. The mirror symmetry of each monomer is broken in structure A, but is preserved in structure B. The two structures are best distinguished by the fact that two chemically inequivalent NMR signals arising from a single type of proton are either present in the same dissymmetric subunit (structure A) or in two different subunits (structure B). In structure A the two chemically different glycoluril protons are 3.0 Å from each other, while in structure B the two chemically different glycoluril protons are greater than 9.0 Å apart. The presence of an NOE contact (observed by 2D-ROESY) between the two signals arising from glycoluril protons eliminates structure B as a possibility (Figure 5C). The ROESY spectrum also displayed 24 other NOE contacts that support the assigned capsular structure of $\mathbf{1_4}$.

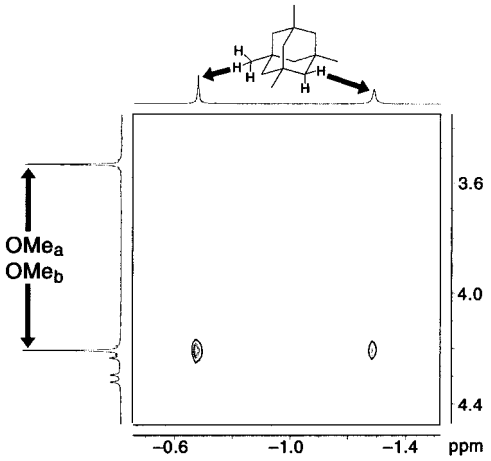

Figure 4. 2D ROESY of complex $\mathbf{1_4}$·**12**. Through-space NOE contact is observed between upfield signals for encapsulated **12** and only one of the two methoxyl signals of the assembly.

Monomer **1** proved to be an avid self-assembler as it forms the tetrameric capsule in a variety of noncompetitive solvents, and it promiscuously encapsulates a number of guest molecules. Formation of the tetramer around those guest molecules listed in Table 1 was observed in CD_2Cl_2, $CDCl_3$, CCl_4, benzene-d_6, toluene-d_8, and *p*-xylene-d_{10}. This behavior is in stark contrast to that observed for compound **2** that lacks only the methoxyl

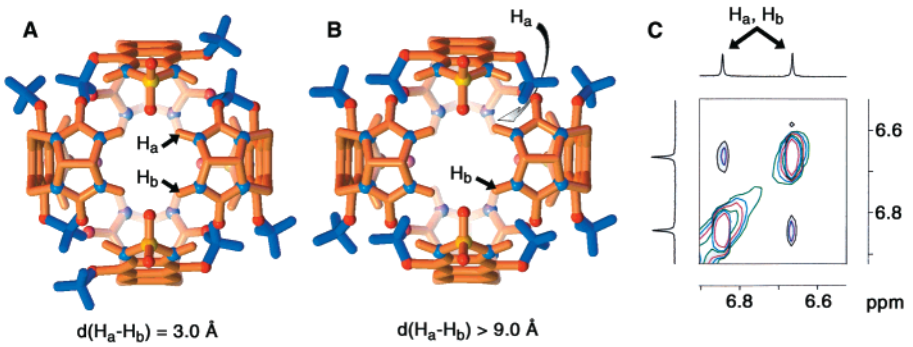

Figure 5. Possible structures for complex $\mathbf{1}_4$ from 1D NMR and molecular modeling. (A) Structure A is comprised of methoxyls in a pinwheel in−out arrangement around the equator. No mirror axes are present. Chemically different glycoluril protons H_a and H_b are calculated to be 3.0 Å apart. (B) Structure B has monomers in two distinct conformations and contains two mirror planes. Chemically different glycoluril protons H_a and H_b have a calculated separation of >9.0 Å. (C) 2D ROESY of complex $\mathbf{1}_4$·**12**. Through space NOE contacts between H_a and H_b (off diagonal) eliminate structure B. Some hydrogen atoms and substituents have been omitted for clarity.

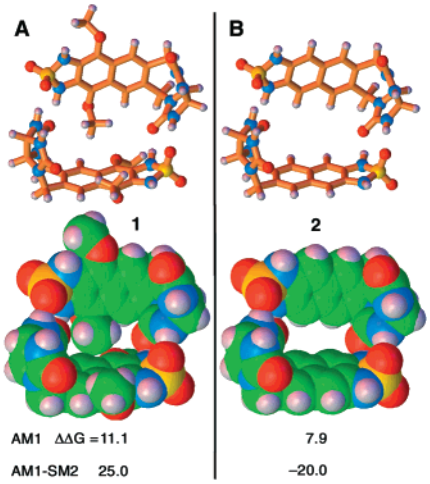

Figure 6. Ball-and-stick and space-filling representations of dimers cut away from minimized tetrameric structures of $\mathbf{1}_4$ and $\mathbf{2}_4$. The presence of methoxyl groups results in more efficient space filling in assemblies of **1** than in assemblies of **2**. The gap visible between adjacent monomers of **2** is at least 1.0 Å wide, as estimated by the subtraction of van der Waals radii from the hydrogen atom to hydrogen atom distance (3.90 Å) measured in models of the tetramer $\mathbf{2}_4$. Semiempirical energies of interaction for the *pairs* of molecules are listed. Some substituents have been omitted for clarity.

substituents on the aromatic spacer. Quite unexpectedly, we found no self-assembled capsules under any of the conditions listed above. Molecular mechanics calculations were used to estimate the geometry of the lowest-energy conformations for the unfilled tetrameric assemblies $\mathbf{1}_4$ and $\mathbf{2}_4$. The interaction energy of two adjacent monomers was then calculated at the semiempirical level for both dimeric structures (Figure 6).[8] In agreement with experiment, the calculations show more favorable self-interaction energy for compound **1** than for compound **2**. We attribute the differences in behavior for these two compounds to the effect of the methoxyl groups on the electronic character of the hydrogen-bonding functions as well as the presence of favorable van der Waals interactions between an inwardly directed methoxyl group and the neighboring aromatic ring.

The tetramer of **2** has a peculiarity that we have not yet encountered in assemblies or in other types of molecular recognition. It has neither face-to-face nor edge-to-face interactions but has edge-to-edge arrangements of its aryl surfaces *at right angles* (Figure 6B). It is unlikely that this is favorable,[9] and it is tempting to hold it responsible for the failure of **2** to carry out its intended function.

Capsule and Guest Dynamics

Direct study of the assembly process for capsules self-assembled through hydrogen bonds is complicated by the broad and complex nature of the disassembled state in NMR spectra. The presence of an assembly-dependent symmetry-breaking process allows us to carry out studies of capsule dynamics, since the complete disassembly of the capsule must be accompanied by the return of free monomers to a symmetric state. The rate of exchange between symmetry-inequivalent protons can be used as an effective probe of the disassembly process.[10] Spin-polarization transfer experiments (EXSY)[11] were used to monitor the dynamics of the complex of **12** and tetramer $\mathbf{1}_4$. The rate of capsule dissociation for complex $\mathbf{1}_4$·**12** in CD_2Cl_2 and CCl_4 was examined by the selective polarization of various signals and the observation of polarization transfer to partner signals differentiated only by the symmetry-breaking caused by assembly. Chemical exchange for any signals assigned to the capsule was *not* observed over 500 ms at temperatures up to 5° below the boiling point of each solvent. Using the value of 343 K (in CCl_4), and the time scale of the experiment[12] (500 ms), the *lower limit* for the activation energy of capsule dissociation to free monomer can be estimated at 20 kcal/mol.

Similar experiments were used to monitor the dynamics of guest exchange processes in the complex $\mathbf{1}_4$·**12**. In CD_2Cl_2, the transfer of spin polarization from free guest to encapsulated guest was observed to occur at a rate of $\sim$10 s^{-1} at 295 K. Conversely, in CCl_4, exchange was not observed to occur within the time frame of the experiment ($k \leq 2$ s^{-1}). This result highlights the role of the solvent in guest-exchange processes.

(8) Semiempirical calculations were carried out using Spartan and MacSpartan: Wavefunction, Inc., 18401 Von Karman Ave., Ste. 370, Irvine, CA 92612.

(9) Jorgensen, W. L.; Severance, D. L. *J. Am. Chem. Soc.* **1990**, *112*, 4768−4774.

(10) (a) Szabo, T.; Hilmersson, G.; Rebek, J., Jr. *J. Am. Chem. Soc.* **1998**, *120*, 6193−6194. (b) Pons, M.; Molins, M. A.; Millet, O.; Bohmer, V.; Prados, P.; De Mendoza, J.; Veciana, J.; Sedo, J. NATO Advanced Study Institute Series C; Plenum: New York, 1999; Vol. 526, pp 67−82.

(11) (a) Perrin, C. L.; Dwyer, T. J. *Chem. Rev.* **1990**, *90*, 935−967. For the study of guest-exchange processes, see: (b) Cai, M.; Sidorov, V.; Lam, Y.-F.; Flowers, R. A.; Davis, J. T. *Org. Lett.* **2000**, *2*, 1665−1668. For the study of conformational dynamics, see: (c) Kelly, T. R.; Tellitu, I.; Sestelo, J. P.; *Angew. Chem., Int. Ed. Engl.* **1997**, *36*, 1866−1868.

(12) The natural relaxation (without transfer) of spin polarization for these signals occurs in 500−1000 ms, placing an upper limit on the time scale of this experiment.

Along with the difference in solvent polarity (and its effect on hydrogen bond strength), the nature of the solvent-filled capsule has been shown to play an important role in guest-exchange processes.[13]

These results show that guest exchange occurs without complete dissociation of the assembly, or even exchange of the "in" and "out" methoxyl substituents. Two mechanisms for guest exchange are consistent with this result. In the first, either a single or two adjacent monomers swing open *without dissociating* to create a door in the assembly. When these doors close, the methoxyls must return to their initial positions to fit into the alternating folded pattern maintained by the monomers that remain intact. This mechanism is reminiscent of guest exchange in the softball family of dimeric capsules.[13] A second pathway involves dissociation of the tetramer into two identical dimers. Here, the hydrogen-bound edge of the dimer locks the bridging methoxyl groups in place. The symmetry considerations of the process are subtle; unlike the tetramer, the dimers are chiral, and dissociation yields either of a pair of two identical enantiomers.

The specific mechanism is less important than its consequences and more difficult to determine. The tetramer $\mathbf{1}_4$ possesses conformational stability that persists for multiple guest exchanges. We have recently reported an encapsulation complex in which hydrogen bonds maintain the imprint of a long-departed chiral guest template.[14] Tetrameric assemblies are capable of generating great diversity,[2b] and the possible extension of molecular imprinting to these systems holds much promise.

Conclusions

As with **2**, the degrees of freedom available to **1** are few; the main skeleton is largely rigid, and the hydrogen-bonding preferences are well established. Despite this simplicity, from the presence of two lowly methoxyl groups emerges self-organization, encapsulation of guest molecules, unexpected symmetry, and conformational memory. The "folding" of this assembly and the dynamics of its substrate binding defy prediction and reasonably reflect the state of the art in supramolecular chemistry; yet the complexity of these processes pales in comparison to the conformational changes and self-organization performed by an enzyme while executing its function.

Experimental Section

General. ^{1}H NMR (600 MHz) and ^{13}C NMR (151 MHz) spectra were recorded on a Brüker DRX-600 spectrometer. Infrared spectra were recorded on a Perkin-Elmer Paragon FT-IR spectrometer. Matrix-assisted laser desorption/ionization FTMS experiments were performed on an IonSpec FTMS mass spectrometer. Electrospray MS experiments were performed on a single-quadrupole Perkin-Elmer API-100 Sciex mass spectrometer. Dichloromethane and THF were passed through columns of activated aluminum oxide as described by Grubbs and co-workers before use.[15] Column chromatography was carried out using silica gel 60 (35−75 μm) as purchased from EM Science. All reagents and solvents were used as purchased from Aldrich Chemicals unless otherwise indicated.

Calculations. Molecular mechanics calculations were carried out using the AMBER* force field as implemented by Macromodel version 6.5.[5] Calculations at the semiempirical level were carried out using Spartan.[8] Cavity volumes were calculated using GRASP.[5]

Encapsulation Studies. ^{1}H NMR (600 MHz) experiments were carried out on a Brüker DRX-600 spectrometer. Deuterated solvents were used as purchased from Cambridge Isotope Labs. Guest molecules were used as purchased from Aldrich, except 1,3,5,7-tetramethyladamantane **(12)**, which was synthesized as previously reported.[16] 1D encapsulation experiments were carried out with a monomer concentration of 2 mM and guest concentrations as noted. The binding constant (K_{app}) of **12** was determined by direct integration of free and bound guest signals for a sample containing 1 equiv of **12** with respect to the tetrameric capsule. All other binding constants were determined by competition experiment.[7] 2D correlation experiments and 1D exchange experiments were carried out on samples with a monomer concentration of 10 mM and guest concentrations of 37.5 mM (15 equiv with respect to tetramer). Kinetics of proton exchange were determined by monitoring spin polarization transfer using a 180° pulse-delay-observe sequence,[11] varying the mixing time from 5 μs to 500 ms.

Synthesis. Cyclic Sulfinate (4). To a mixture of the dibromide **3** (235 mg, 0.380 mmol) and tetra-*n*-butylammonium bromide (24 mg, 0.076 mmol) in anhydrous DMF (7 mL) cooled to 0 °C was added Rongalite (132 mg, 0.855 mmol, Acros Organics) as a solid. Stirring was continued for 7 h at 0 °C, and the reaction was allowed to warm to room temperature and stirred overnight. The reaction was poured into water (25 mL) and extracted gently with Et_2O (6 × 15 mL). The combined organic extracts were dried over Na_2SO_4 and concentrated to give the product (195 mg, 98%) as a white solid which was used without further purification. ^{1}H NMR ($CDCl_3$) δ 1.61 (s, 18H), 3.56 (d, 1H, J = 7.0 Hz), 3.75 (s, 3H), 3.78 (s, 3H), 4.41 (d, 1H, J = 7.0 Hz), 5.17 (AB qr, 2H, J = 18.9, 14.3 Hz). ^{13}C NMR ($CDCl_3$) δ 27.92, 50.62, 57.85, 60.99, 61.15, 87.29, 119.68, 119.93, 120.27, 126.91, 142.66, 144.56, 146.42, 146.46. IR ($CHCl_3$ cast) cm^{-1} 2984.9, 2938.5, 1766.0, 1480.7, 1448.9, 1396.4, 1372.0, 1293.8, 1245.4, 1141.6, 1074.0, 840.7, 757.6. MS (ESMS; MNa^+) calcd for $C_{20}H_{28}N_2O_{10}S_2Na$ 543, found 543.

Naphthalene Diester (6). Sulfinate **4** (195 mg, 0.375 mmol), dimethylacetylenedicarboxylate (160 mg, 1.125 mmol), and benzene (6 mL) were combined and heated at reflux for 2 h. DDQ (213 mg, 0.938 mmol) was added and reflux continued for 2 h. The reaction was concentrated to dryness, and the residue was chromatographed over silica gel (CH_2Cl_2) and triturated with MeOH to give the product as a white solid (153 mg, 69%). ^{1}H NMR ($CDCl_3$) δ 1.63 (s, 18H), 3.91 (s, 6H), 3.96 (s, 6H), 8.56 (s, 2H). ^{13}C NMR ($CDCl_3$) δ 27.89, 53.04, 61.25, 87.22, 118.63, 124.85, 127.71, 129.32, 141.14, 145.76, 168.02. IR ($CHCl_3$ cast) cm^{-1} 2981.8, 2945.5, 1758.5, 1728.3, 1426.4, 1275.5, 1239.2, 1136.6, 1112.45. MS (ESMS; MNa^+) calcd for $C_{26}H_{32}N_2O_{12}$-SNa 619, found 619.

Naphthalene Diol (7). Naphthalene diester **(6)** (304 mg, 0.51 mmol) was dissolved in CH_2Cl_2 and cooled to 0 °C. DIBAL (2.5 mL, 2.5 mmol) in toluene was added over 90 s, and the reaction was stirred at 0 °C for 2.5 min before adding EtOAc (5 mL) and water (5 mL) to quench the reaction. Addition of THF (20 mL) and 1 N NaOH (10 mL) gave a separable mixture. The organic layer was washed with brine (3 × 10 mL), and the organic extracts were dried over Na_2SO_4 and concentrated to dryness. Chromatography over silica gel (3:7 hexanes: EtOAc) yielded the product as a colorless oil (137 mg, 50%). ^{1}H NMR ($CDCl_3$) δ 1.63 (s, 18H), 3.30 (s, 2H), 3.87 (s, 6H), 4.86 (s, 2H), 8.11 (s, 2H). ^{13}C NMR ($CDCl_3$) δ 27.93, 61.02, 64.59, 86.76, 116.83, 123.25, 127.26, 138.16, 140.89, 146.14. IR ($CHCl_3$ cast) cm^{-1} 3608−3140 (br), 2984.3, 2938.5, 1764.8, 1620.4, 1428.2, 1395.9, 1371.6, 1296.6, 1246.6, 1096.3, 755.7. MS (ESMS; MNa^+) calcd for $C_{24}H_{32}N_2O_{10}SNa$ 563, found 563.

Naphthalene Dibromide (8). Naphthalene diol **(7)** (180 mg, 0.33 mmol) was dissolved in dry THF (5 mL), and carbon tetrabromide (552 mg, 1.66 mmol) was added followed by triphenylphosphine (437 mg, 1.66 mmol). After stirring at room temperature for 18 h the reaction was filtered through Celite and concentrated to dryness. Column chromatography (1:1 hexanes:EtOAc) yielded the product as a colorless oil (167 mg, 75%). ^{1}H NMR ($CDCl_3$) δ 1.65 (s, 18H), 3.91 (s, 6H), 4.88 (s, 4H), 8.20 (s, 2H). ^{13}C NMR ($CDCl_3$) δ 27.95, 30.79, 61.08,

(13) Santamaria, J.; Martín, T.; Hilmersson, G.; Craig, S. L.; Rebek, J., Jr. *Proc. Natl. Acad. Sci. U.S.A.* **1999**, *96*, 8344−8347.

(14) Rivera, J. M.; Craig, S. L.; Martín, T.; Rebek, J., Jr. *Angew. Chem., Int. Ed.* **2000**, *39*, 2130−2132.

(15) Pangborn, A. B.; Giardello, M. A.; Grubbs, R. H.; Rosen, R. K.; Timmers, F. J. *Organometallics* **1996**, *15*, 1518−1520.

(16) Bolestova, G. I.; Parnes, Z. N.; Kursanov, D. N. *Zh. Org. Khim.* **1983**, *19*, 339−343.

86.94, 117.50, 125.54, 127.55, 135.00, 140.79, 145.99. IR ($CHCl_3$ cast) cm^{-1} 2976.1, 2928.2, 1765.95, 1426.8, 1293.7, 1245.4, 1140.7, 1096.8. MS (ESMS; MNa^+) calcd for $C_{24}H_{30}N_2O_8SNa$ 689, found 689.

Boc-Protected Monomer (10). *n*-Heptylphenyl glycoluril **(9)**[4] (166 mg, 0.338 mmol) was dissolved in hot DMSO (5 mL) and THF (2 mL) and the temperature maintained at 85 °C. Freshly powdered KOH (45 mg, 0.675 mmol) was added and the heating continued for 20 min, resulting in a clear solution. The heat was removed, and immediately a solution of the naphthalene dibromide **(8)** (45 mg, 0.068 mmol) in THF (1 mL) was added dropwise and washed forward with THF (0.5 mL). The resulting mixture was allowed to cool to room temperature and stirred for 2 h. The reaction was poured onto water (50 mL) and filtered. The resulting solid was washed with CH_2Cl_2 (20 mL), and the filtrate was then concentrated to dryness. Column chromatography (1:1 hexanes:EtOAc) yielded the product as a white solid (14.6 mg, 22%). ^{1}H NMR (THF-d_8) δ 0.90 (t, 6H, J = 6.8 Hz), 1.3−1.1 (m, 16 H), 1.47 (m, 4H), 1.60 (s, 18H), 2.42 (t, 2H, J = 7.6 Hz), 2.47 (t, 2H, J = 7.6 Hz), 3.90 (s, 6H), 4.30 (d, 2H, J = 15.3 Hz), 4.99 (d, 2H, J = 15.3 Hz), 6.84 (d, 2H, J = 8.1 Hz), 6.98 (d, 2H, J = 8.2 Hz), 7.07 (d, 2H, J = 8.2 Hz), 7.11 (d, 2H, J = 8.1 Hz), 7.19 (s, 2H), 8.11 (s, 2H). ^{13}C NMR (THF-d_8) δ 14.6, 23.8, 28.0, 30.1, 30.3, 32.5, 32.6, 33.0, 36.2, 36.4, 45.8, 61.3, 86.3, 118.0, 124.0, 127.7, 128.4, 128.5, 129.2, 129.4, 133.5, 137.1, 137.6, 142.3, 143.6, 144.2, 147.1, 159.5. IR ($CHCl_3$ cast) cm^{-1} 3241.0 (br), 2927.4, 2851.3, 1765.9, 1694.2, 1462.7, 1425.6, 1292.7, 1240.8, 1142.6, 945.5. MS (ESMS; M − H^-) calcd for $C_{54}H_{69}N_6O_{10}S$ 993, found 993.

Naphthalene Dimethoxy Tetramer (1). The Boc-protected monomer **(10)** (19.6 mg, 19.6 μmol) was dissolved in dry CH_2Cl_2 (3 mL), and trifluoroacetic acid (1 mL) was added at room temperature. After stirring for 4 h, the reaction was concentrated to dryness on a rotary evaporator and chromatographed over silica gel (3−10% MeOH in CH_2Cl_2) to give the product as a buff-colored solid (12.4 mg, 79%). ^{1}H NMR (THF-d_8) δ 0.90 (t, 6H, J = 6.0 Hz), 1.31−1.19 (m, 16H), 1.47 (m, 4H), 2.42 (t, 2H, J = 7.6 Hz), 2.46 (t, 2H, J = 7.6 Hz), 3.91 (s, 6H), 4.24 (d, 2H, J = 15.3 Hz), 4.93 (d, 2H, J = 15.5 Hz), 6.84 (d, 2H, J = 8.2 Hz), 6.97 (d, 2H, J = 8.2 Hz), 7.05 (d, 2H, J = 8.2 Hz), 7.10 (d, 2H, J = 8.2 Hz), 7.10 (s, 2H), 7.91 (s, 2H), 10.09 (s, 2H). ^{13}C NMR (THF-d_8) δ 14.60, 23.77, 30.11, 30.27, 30.30, 30.83, 32.52, 32.64, 33.01, 33.03, 36.25, 36.39, 45.95, 61.03, 79.17, 88.83, 122.74, 123.44, 124.73, 128.37, 128.54, 129.20, 129.35, 133.61, 135.28, 135.51, 137.23, 143.55, 144.05, 159.50. IR ($CHCl_3$ cast) cm^{-1} 3398.3, 3312.8, 2923.9, 2852.6, 2687.2, 1693.7, 1643.8, 1468.9, 1328.4, 1256.9, 1168.0, 1107.1, 1055.2. HRMS (MALDI-FTMS; MH^+) calcd for $C_{44}H_{55}N_6O_6S$ 795.3998, found 795.3866.

Naphthalene Tetramer (2). Synthesis of this compound was achieved from known dibromide **11** by transformations analogous to those used in the synthesis of **1**. ^{1}H NMR (THF-d_8) δ 0.89 (t, 6H, J = 6.0 Hz), 1.30 (m, 36H), 1.47 (m, 4H), 2.44 (m, 4H), 4.21 (d, 2H, J = 15.3 Hz), 4.92 (d, 2H, J = 15.3 Hz), 6.85 (d, 2H, J = 8.1 Hz), 6.91 (s, 2H), 6.98 (d, 2H, J = 8.1 Hz), 7.06 (d, 2H, J = 8.1 Hz), 7.12 (d, 2H, J = 8.1 Hz), 7.20 (s, 2H), 7.64 (s, 2H), 9.91 (s, 2H). ^{13}C NMR (THF-d_8) δ 14.62, 23.75, 30.21, 30.31, 30.52, 30.67, 30.82, 30.87, 30.89, 32.54, 32.65, 33.06, 36.28, 36.40, 45.81, 79.41, 89.10, 106.25, 128.43, 128.50, 128.53, 129.20, 129.37, 130.03, 131.79, 133.45, 134.61, 137.00, 143.66, 144.13, 159.97. HRMS (MALDI-FTMS; M − H^-) calcd for $C_{52}H_{69}N_6O_4S$ 873.5106, found 873.5068.

Acknowledgment. This research was supported by the Skaggs Research Foundation and the NIH. For fellowship support F.H. thanks NSERC, C.N. and S.L.C. thank the NIH, and T.M. thanks The Ministerio de Educación y Cultura of Spain.

JA002340Q